

GAS-FILLED TARGET DESIGNS PRODUCE IGNITION-SCALE PLASMA CONDITIONS WITH NOVA

<i>L. V. Powers</i>	<i>B. H. Failor</i>	<i>B. J. MacGowan</i>	<i>R. E. Turner</i>
<i>P. A. Amendt</i>	<i>S. W. Haan</i>	<i>D. S. Montgomery</i>	<i>E. A. Williams</i>
<i>R. L. Berger</i>	<i>J. A. Harte</i>	<i>D. H. Munro</i>	<i>B. H. Failor</i>
<i>C. A. Back</i>	<i>D. H. Kalantar</i>	<i>S. M. Pollaine</i>	<i>J. C. Fernandez</i>
<i>T. P. Bernat</i>	<i>R. L. Kauffman</i>	<i>T. D. Shepard</i>	<i>W. W. Hsing</i>
<i>K. G. Estabrook</i>	<i>B. F. Lasinski</i>	<i>L. J. Suter</i>	<i>B. H. Wilde</i>

Introduction

In current hohlraum target designs for the National Ignition Facility (NIF), low- Z gas fills are used to reduce radial expansion of the gold hohlraum wall.¹ In vacuum, the expansion of the hohlraum wall during the NIF laser pulse (~ 18 ns) would produce unacceptable levels of asymmetry in the radiation field. The gas, once heated, provides enough pressure to tamp the radiating gold surface. In current designs, the H/He gas fill produces a plasma with an electron density of nearly 10^{21} cm $^{-3}$ and an electron temperature in excess of 3 keV at the peak of the laser pulse. The laser beams propagate efficiently through the weakly absorbing hot gas and deposit most ($\sim 90\%$) of their energy in the gold wall near the initial radius of the target, thus maintaining the high radiation symmetry required for imploding high-convergence capsules.

Even for low-density ($n_e \approx 0.1n_c$) fills, however, the linear gain for stimulated Brillouin scattering (SBS) in the gas is high. In smaller-scale exploding-foil targets,² flow velocity gradients typically limit the SBS gain to modest values. At the peak of the NIF laser pulse, the laser beam must propagate through 2–3 mm of gas plasma with a calculated velocity-gradient scalelength of $L_v \approx 10$ mm. Velocity-gradient stabilization is ineffective at this scale, and the (linear) SBS gain is set by ion Landau damping. For the peak (single beam) NIF intensity of 2×10^{15} W/cm 2 and the calculated plasma conditions, the linear SBS gain coefficient in the gas plasma is ~ 20 . Although nonlinear effects are likely to limit the SBS reflectivity,³ the scaling of such mechanisms is not quantitatively understood.

Although numerous experimental studies of scattering instabilities in laser-produced plasmas have been performed,⁴ plasma conditions of NIF target designs are not easily accessible with current lasers. Further, difficulty in quantitatively modeling SBS in past experiments casts doubt on theoretical extrapolation. The objective of the work reported here is to design targets for interaction experiments that match as closely as possible the conditions of the NIF gas plasma in the path of the laser beams. To assess SBS scaling to NIF parameters, we have designed Nova targets that closely mimic the NIF gas plasma parameters and that allow scaling studies in density, temperature, and laser conditions. Gas-filled targets are heated with nine beams of the Nova laser to produce large, hot, nearly static plasmas. These plasmas have been extensively characterized using x-ray imaging and spectroscopy to verify the plasma conditions.^{5–7} Calculations of the plasma conditions compare favorably with these measurements. In interaction experiments,^{8,9} the qualitative features of the backscattered spectra¹⁰ from the tenth Nova beam are also consistent with the calculated plasma conditions and temporal evolution of the target parameters that influence SBS.

Although the primary focus of this work was to design and field targets that reproduce NIF underdense plasma parameters important to SBS, the target designs have also proven useful for ongoing studies of other parametric processes that could affect NIF. The gains for stimulated Raman backscattering (SRS) in these plasmas are also high and comparable to calculated SRS gains in NIF hohlraums. New diagnostic capabilities have led to experiments to study the scaling

of SRS backscattering with electron temperature, electron density, and beam conditioning.¹¹ Broadening of SRS spectra from unsmoothed beams is interpreted as evidence that filamentation is above threshold but is suppressed by beam smoothing in agreement with calculations.¹² In other experiments, Brillouin forward scattering in crossed beams is being investigated using these target designs.¹³

NIF Target Analysis

We have analyzed detailed simulations of various NIF target designs¹ using the LASNEX ICF design code¹⁴ to define desirable conditions for Nova preformed-plasma experiments. To assess the potential levels of scattering instabilities in NIF plasmas, we have calculated the linear gain and the resultant reflectivities by assuming no nonlinear saturation effects other than pump depletion and by assuming that the reflection is confined within the solid angle of the incident light.

Figure 1 shows the target geometry and a typical laser pulse shape for the baseline NIF hohlraum design. In NIF indirect-drive target designs, the hohlraum wall is illuminated by two pairs of symmetrically placed rings of laser beams. The hohlraum is filled with He or H/He mixtures at an initial density of 0.0013 g/cm^3 , which corresponds to an electron density $n_e = 4 \times 10^{20} \text{ cm}^{-3}$ at full ionization. The density of the low-Z fill plasma evolves throughout the pulse because of wall expansion, plasma blowoff from the capsule, and material loss through the laser entrance holes. We have analyzed simulations for a range of NIF target designs at times throughout the laser pulse. The highest linear gains for SRS and SBS occur at the peak of the pulse, when the maximum intensity of a single beam is $I = 2 \times 10^{15} \text{ W/cm}^2$. Figure 2 shows the calculated profiles for laser intensity I_L , electron density n_e , electron temperature T_e , ion/electron temperature ratio T_i/T_e , and flow velocity component parallel to the beam path $v_{||}$, along the propagation path for the baseline NIF hohlraum design. Alternative designs with lower peak power and correspondingly lower plasma densities at the peak of the pulse result in lower gains for scattering instabilities.

The laser intensity in the NIF point design is well below the threshold for absolute SRS at the calculated densities and temperatures, so only the convective instability is a concern. To obtain the small-signal intensity gain coefficient $G(\omega_s)$ for SRS, we integrate the local intensity spatial gain rate¹⁵ $\kappa(\omega_s, z)$ over the path of the scattered light. Using plasma profiles from LASNEX simulations, we evaluate

$$\kappa(\omega_s, z) = \frac{(k_0 - k_s)^2 v_0^2}{4\omega_0 v_g} \text{Im} \left[\frac{(1 + \chi_i)\chi_e}{1 + \chi_i + \chi_e} \right] \quad (1)$$

on a fine mesh along the propagation path of the laser beam. Here z is the position along the ray path, $\omega_{0,s}$ and $k_{0,s}$ are the frequency and wavenumber of the pump and scattered light waves, respectively, $v_0 \equiv eE_0/m\omega_0$ is the laser pump strength parameter, $v_g \equiv c_s^2 k_s/\omega_s$ is the group velocity of the ion acoustic wave (c_s is the sound speed in the plasma), and $\chi_{e,i}$ are the electron and ion susceptibilities, respectively. The gain calculation includes a multi-species treatment of ion Landau damping.¹⁶ The intensity variation along the ray path due to beam divergence and inverse bremsstrahlung absorption is also included.

The propagation length through the $\sim 0.1n_c$ gas plasma is longer for the inner beam cone, resulting in higher integrated SRS gain. At NIF scale, flow velocity gradients are weak in the direction of beam propagation ($L_v \approx 10 \text{ mm}$) and do not effectively limit SRS. On the other hand, the ions and electrons are near equilibrium ($T_i/T_e = 0.4$) at the high-intensity peak of the pulse, leading to efficient ion Landau damping by the light

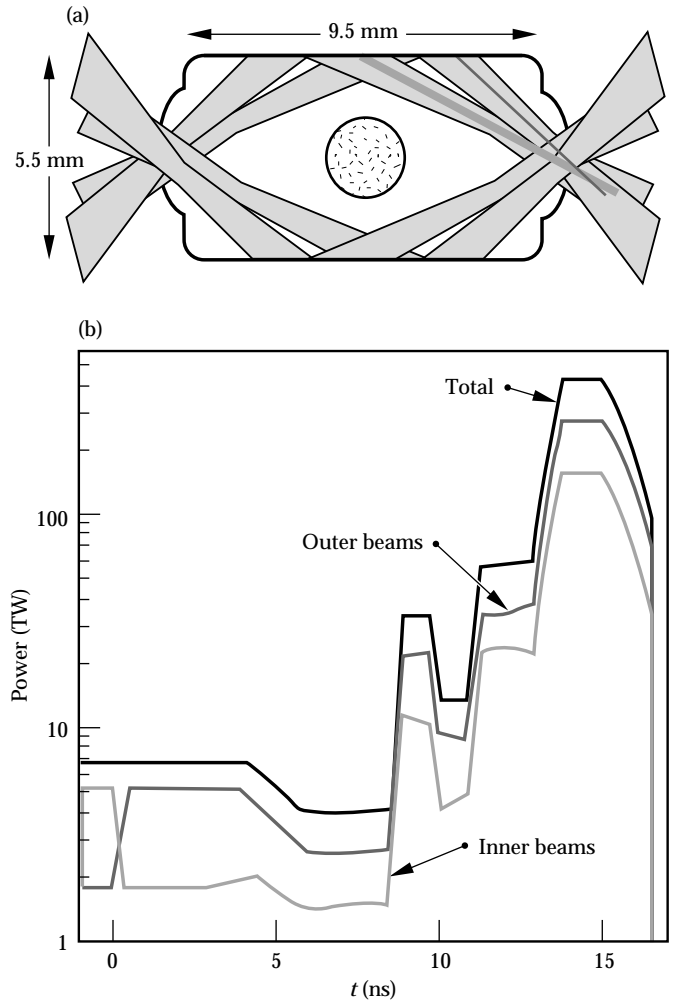


FIGURE 1. NIF target design. (a) Target and illumination geometry for baseline NIF hohlraum design. (b) Typical laser pulse shape. (50-04-1095-2377pb02)

ions in the gas. In this parameter regime, the linear gain exponent for SRS is approximately

$$G_{\text{SBS}} = \pi \times 10^{-16} \left(\frac{I^2}{T_e} \right) \left(\frac{n_e}{n_c} \right) \left(\frac{\omega_a}{v_i} \right) \left(\frac{L}{\lambda} \right), \quad (2)$$

where I is the laser intensity in W/cm^2 , λ is the laser wavelength in micrometers, T_e is the electron temperature in keV, n_e/n_c is the electron density normalized to critical density, and ω_a and v_i are the ion-acoustic-wave

frequency and amplitude damping rate, respectively. Landau damping increases further when the He fill is replaced by a H/He mixture with the same electron density.¹⁶ For pure He fill, the calculated linear gain exponents for SRS for the inner and outer beams are 28 and 9, respectively; for an equimolar H/He mixture, the corresponding values are 21 and 6. The longer gas path length and lower electron temperature in the inner cone also lead to higher SRS gain.

For the high gain exponents calculated for the inner beam cone, linear theory is not adequate to assess

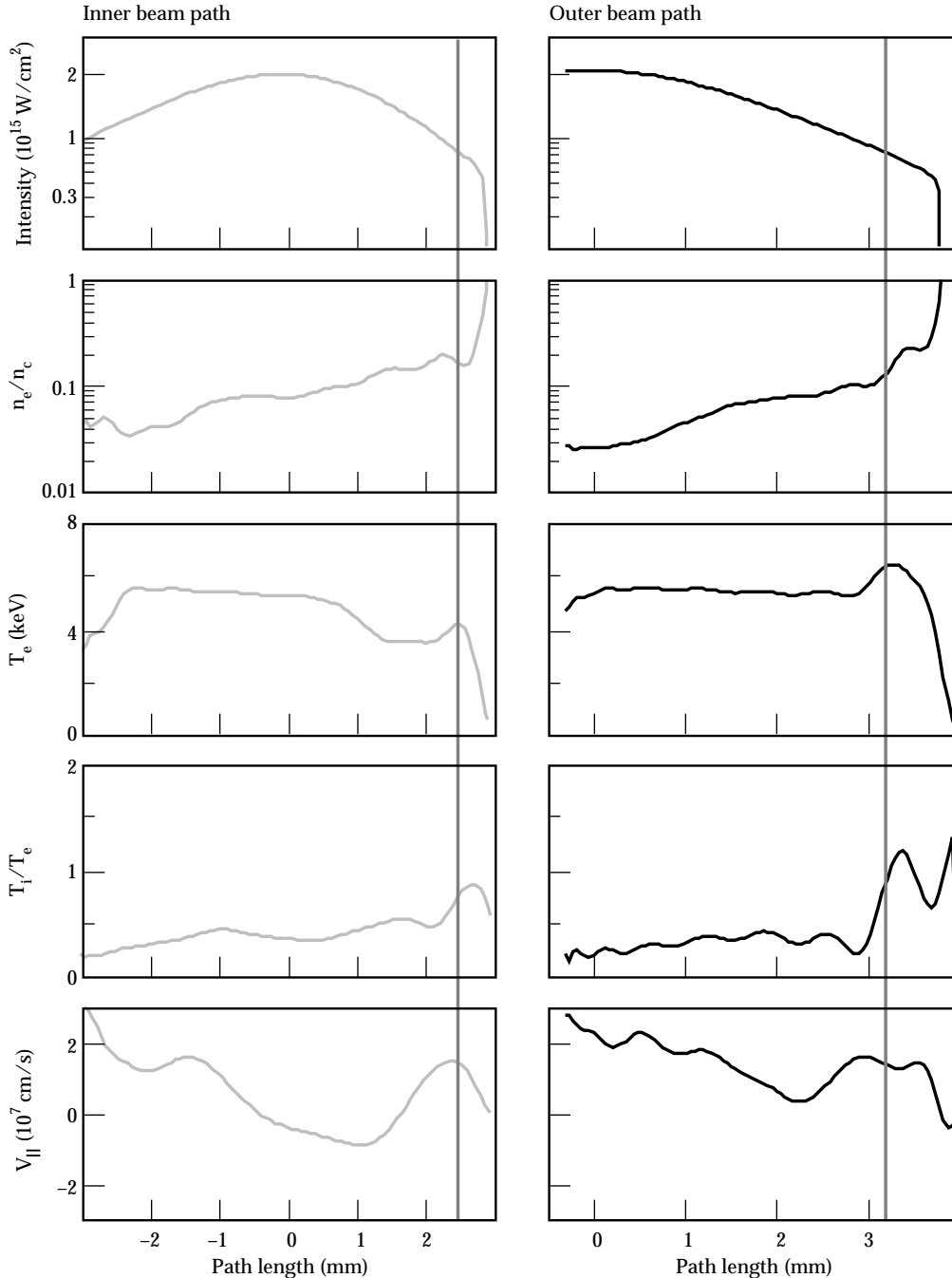


FIGURE 2. NIF plasma parameters: lineouts of intensity, electron density, electron temperature, ion/electron temperature ratio, and flow velocity parallel to the laser path for the inner (left) and outer (right) beam cones along the paths indicated by gray lines in Fig. 1. The laser entrance hole is at the left limit of the plots; the gas/gold interface is marked by light shaded vertical lines. The path length is defined such that the position of best focus of the laser beam is at zero. (50-04-1095-2378pb02)

scattering levels. Nonlinear damping or detuning of SBS-produced ion waves is likely to limit the instability growth to much lower levels.³ However, the intensity structure of spatially smoothed laser beams, although an improvement over that of unsmoothed Nova beams, increases the effective gain above that for a uniform beam.¹⁷ Temporal beam smoothing is therefore necessary to reduce the expected gain.¹⁸ Although all these effects are expected to be important, quantitative predictions of scattering levels including these effects is beyond the scope of current simulation techniques. Interaction experiments using the Nova targets described below have provided a means for quantifying scattering levels in plasmas similar to the low- Z fill plasma in NIF hohlraum designs and for verifying that scattering levels in such plasmas are acceptable.

Nova Target Designs

The thermal energy content of the gas plasma in the baseline NIF hohlraum design is >70 kJ at the peak of the pulse, so it is not possible to create a comparable plasma with the ~ 30 kJ available with Nova. Instead, we have endeavored to identify and reproduce the essential parameters of the NIF inner beam path in Nova experiments. First, a large, nearly uniform test plasma is required to provide a comparable plasma path length in which SBS gain is not limited by flow gradients. Second, a relatively hot plasma is required to access the strong damping regime for SRS. Third, the relevant plasma conditions must be maintained for much longer than the growth times for instabilities to assess asymptotic scattering levels. Based on these criteria we set electron density $n_e \approx 10^{21} \text{ cm}^{-3}$, electron temperature $T_e > 3 \text{ keV}$, interaction length $L \approx 2 \text{ mm}$, flow velocity gradient scalelength $L_v > 6 \text{ mm}$, and plasma lifetime $\geq 0.5 \text{ ns}$ as desirable parameters for Nova target designs.

Various target options were investigated in simulations and evaluated against these criteria. The gas targets were selected for three reasons. First, and perhaps most important, is the consideration that the underdense NIF plasma is formed by heating a low-density gas; hence we expect gas targets to closely parallel the NIF plasma formation processes. Second, a substantial amount of Nova's energy would be required to expand a solid target to achieve the long-scalelength plasma required. Third, the initially homogeneous gas fill suggests less uncertainty and temporal variation in the plasma density than plasmas formed by expansion. Two principal target types were used (Fig. 3), both containing neopentane (C_5H_{12}) gas at 1 atm pressure ($n_e = 10^{21} \text{ cm}^{-3}$ at full ionization): (1) gas balloons ("gasbags") ~ 2.5 – 3 mm in diameter with a ~ 5000 -Å thick polyimide ($\text{C}_{22}\text{H}_{10}\text{N}_2\text{O}_5$) membrane, and (2) cylindrical gold hohlraums with length and diameter $\sim 2.5 \text{ mm}$ with polyimide windows $\sim 6000 \text{ Å}$

thick to contain the gas. Denavit and Phillion¹⁹ proposed similar gas target geometries. An alternative hohlraum geometry was used in complementary experiments fielded on Nova by Los Alamos National Laboratory.²⁰ Using nine Nova beams, which deliver $\sim 30 \text{ kJ}$ of $0.351\text{-}\mu\text{m}$ light, we heat the gas to preform plasmas with the desired parameters. The tenth beam, an interaction beam whose intensity, pulse shape, f/number , and spatial and temporal intensity structure ("smoothness") are varied, is delayed until the gas target is expected to be uniformly heated.

The behavior of the two targets is similar, although details differ because of the different geometries and pulse shapes. In both targets the laser beam burns through the polyimide in $\sim 200 \text{ ps}$; the gas becomes transparent by $t \approx 500 \text{ ps}$. The calculated electron density (10^{21} cm^{-3}) and temperature ($\sim 3 \text{ keV}$) of the preformed plasma are uniform over a length of $L \approx 2 \text{ mm}$. The maximum calculated flow velocity in this region is $< 10^7 \text{ cm/s}$. The path length of the $0.1n_c$ density plateau decreases to $\sim 1.5 \text{ mm}$ at $t = 1 \text{ ns}$ because of rarefaction.

In the gasbag targets, heater beams are arranged to symmetrically illuminate nearly the entire target surface [Fig. 3(a)]. The temperature and density in the center of the target is very uniform after the initial plasma formation. In the hohlraum targets, laser access is limited to laser entrance holes in the ends of the cylinder. The beams are therefore more tightly focused than in the gasbag geometry [Fig. 3(b)], and the laser directly heats only a portion of the contained gas. The gas plasma created in the hohlraum targets exhibits a weak

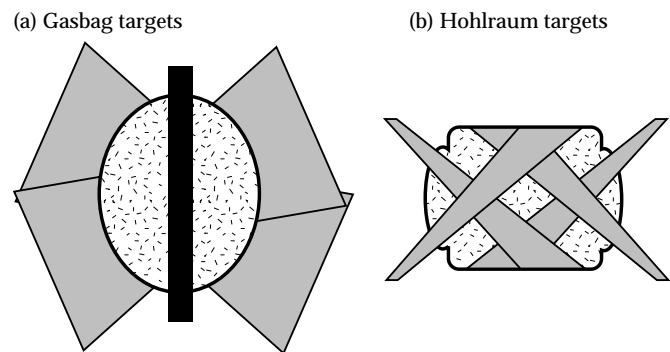


FIGURE 3. Nova target geometries for (a) gasbag and (b) hohlraum targets. For the gasbag target, the dark band indicates the position of the washer. Speckled regions represent gas fill; gray shading shows the illumination geometry for the heating beams. (50-04-1095-2379pb01)

density gradient along the beam path, with density decreasing towards the laser entrance hole. The presence of underdense gold blowoff in the hohlraum may, on the other hand, produce additional SBS. Because most of Nova's energy is required to heat the gas, however, the gold plasma evolution does not approximate

the NIF gold blowoff. SBS from the underdense gold plasma in gas-filled hohlraums is the subject of separate ongoing experiments.

Extensive characterization was carried out to ensure that predicted plasma conditions were achieved. Spectroscopic measurements are consistent with the calculated underdense plasma temperatures.⁵ Imaging techniques confirm the plasma size, homogeneity, and temporal evolution.⁶ Streaked and gated images show that the heater beams propagate through the gas as calculated without significant breakup.⁷ Optical spectra are consistent with expected target parameters and evolution.¹⁰

Comparison of Nova and NIF Target Parameters

Figure 4 shows selected plasma parameters from LASNEX simulations of Nova gas-filled targets and from the baseline NIF hohlraum design. For the Nova targets, quantities are plotted at the time when the peak SBS is observed in interaction experiments (0.9 ns for

gasbag targets and 1 ns for hohlraums). For the NIF targets, quantities are plotted at the peak of the pulse ($t = 14.5$ ns), when the calculated SBS gain is highest. At the time of peak SBS, the Nova targets have a >1.5 mm region of plasma with electron density $\sim 0.1n_c$, flow velocity gradient scalelengths $L_v > 6$ mm, electron temperatures $T_e > 3$ keV, and ion/electron temperature ratios $T_i/T_e \approx 0.15$ – 0.2 . These parameters match the NIF gas plasma conditions within a factor of two.

The calculated linear gain exponents for SBS and SRS backscattering are similar for the Nova targets and the NIF baseline design. Table 1 shows gain exponents for peak laser intensity $I = 2 \times 10^{15}$ W/cm² and $f/8$ focusing, with best focus as defined in Fig. 4. Gains are shown for targets without hydrogen in the fill gas (C_5D_{12} for Nova and pure He for NIF) and for the baseline designs (C_5D_{12} for Nova and equimolar H/He for NIF). The gasbag targets have somewhat higher peak gains than the Nova hohlraum targets for similar fill conditions, primarily because the plasma density is more homogeneous in the gasbags. Both Nova targets have calculated gain exponents comparable to those for the NIF inner cone. Gains for SRS and SBS

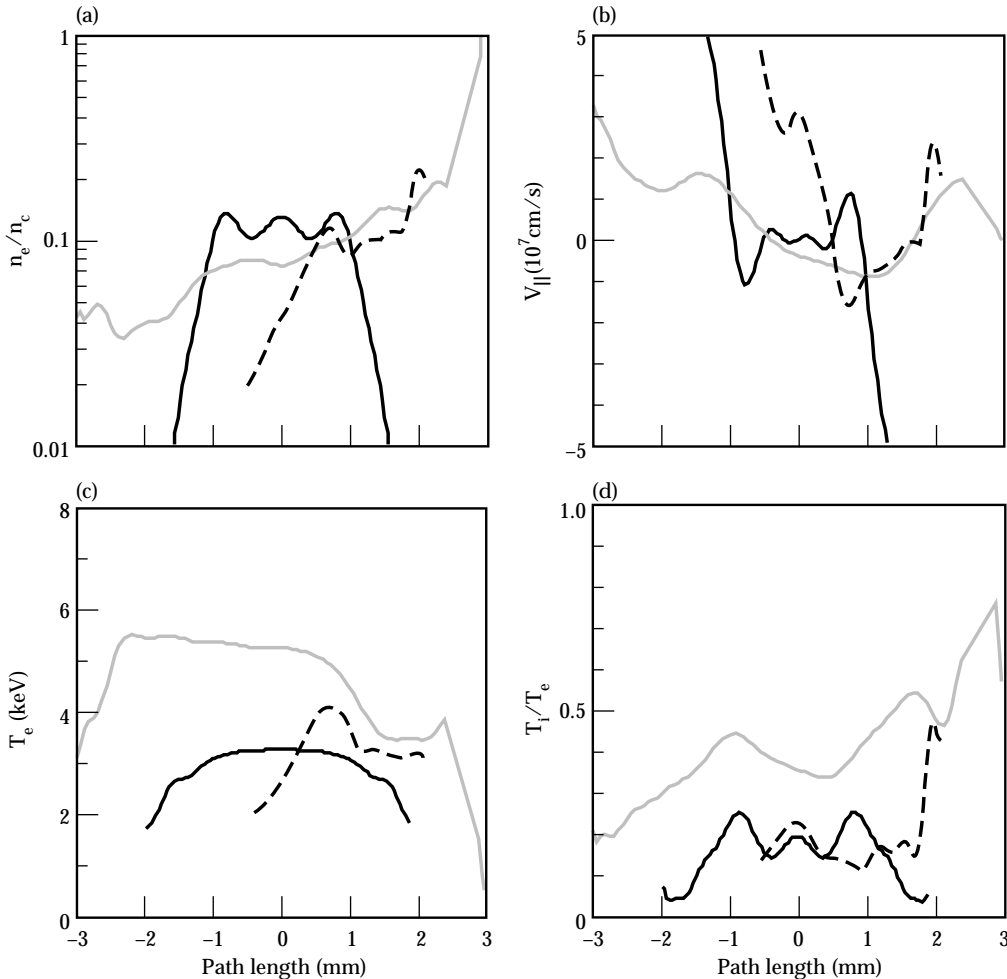


FIGURE 4. Calculated parameters of the low- Z gas plasma along a beam path for the inner cone of NIF beams (gray line), Nova hohlraums (solid line), and gasbags (dashed line). The path length is defined such that the nominal position of best focus of the interaction beam in Nova experiments coincides with best focus of the NIF laser at zero. (50-04-1095-2380pb01)

backscattering are lower for the NIF outer beam cone because of a shorter laser path length through the gas fill plasma. For both instabilities, the longer path length of plasma in the NIF target is compensated for by increased Landau damping to give comparable gains to the Nova targets. For SRS, the higher value of T_i/T_e in the NIF targets leads to increased ion Landau damping. Ion Landau damping is most effective when light (H) ions are present, as shown in Table 1 and as discussed in detail in Refs. 10 and 16. For SRS, electron Landau damping is predicted to be more effective in the NIF target because of the higher electron temperature. Additional scaling experiments have been performed on Nova with higher intensity ($>5 \times 10^{15} \text{ W/cm}^2$) interaction beams,^{8,9} for which the calculated gain exponents exceed NIF values by more than a factor of two.

Calculated backscattering spectra from the Nova targets show features that are signatures of large, static plasmas. Comparisons with observed spectra^{7,10} provide further verification that the calculated plasma conditions have been achieved. Figure 5 shows a typical calculated SRS spectrum from a gasbag target. The interaction beam in the calculations (and in typical

TABLE 1. Calculated linear gain exponents for Nova and NIF target designs.

Target design	SRS	SBS	SBS (no hydrogen)
Nova gasbag	20	35	64
Nova gas hohlraum	16	19	27
NIF (inner cone)	30	21	28
NIF (outer cone)	7	6	9

interaction experiments) is a 1-ns flat-topped pulse with 200 ps rise time, delayed 400 ps relative to the plasma formation laser beams. The brightest feature is red-shifted by $\sim 10 \text{ \AA}$ from the incident wavelength $\lambda_0 = 0.351 \text{ \mu m}$. This corresponds to scattering from the hot, static density plateau in the middle of the target. By contrast, SRS spectra from exploding foils or disks are typically blue-shifted, indicating that the signal is dominated by plasma regions in which $v_{||} > c_s$. The calculated gain decreases after $\sim 1 \text{ ns}$ because of the gradual disassembly of the density plateau and because of energy transfer from the electrons to the ions, which increases the ion Landau damping. These qualitative features are seen in experiments in which significant scattering is observed,^{10,11} although peak scattering occurs somewhat later ($\sim 200 \text{ ps}$) than calculated. Figure 6 shows a typical calculated SRS spectrum. The dominant feature at $\lambda \approx 5700 \text{ \AA}$ is indicative of scattering from the $0.1n_c$ density plateau formed by

the gas. The longer-wavelength feature that appears at $t \approx 1 \text{ ns}$ is associated with a compression shock generated by the expanding polyimide membrane; this feature appears in some of the measured spectra.^{7,10} Again the scattering level decreases after $\sim 1 \text{ ns}$, although the interaction beam is at full intensity until $t \approx 1.4 \text{ ns}$, in qualitative agreement with observations.

Although qualitative features of the backscattered spectra are consistent with the calculated plasma evolution, linear theory is clearly inadequate to model

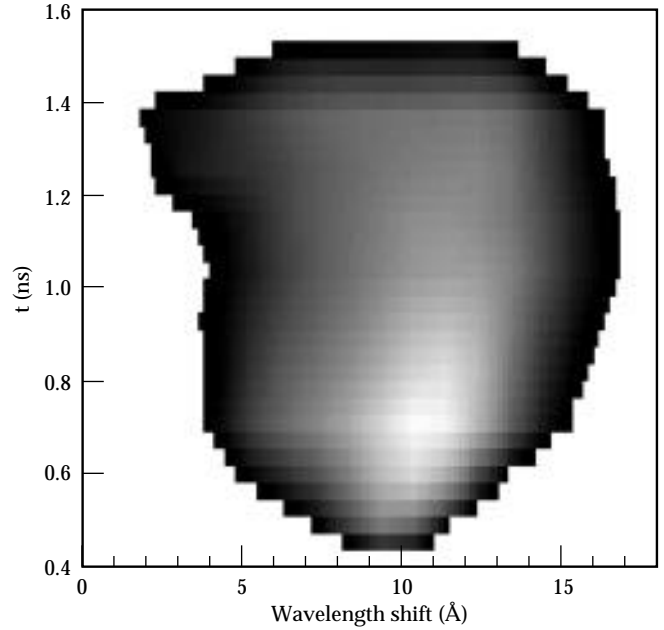


FIGURE 5. Calculated SRS backscattered spectra from a neopentane-filled gasbag target with $f/8$ interaction beam intensity $I = 2 \times 10^{15} \text{ W/cm}^2$. (50-04-1095-2386pb02)

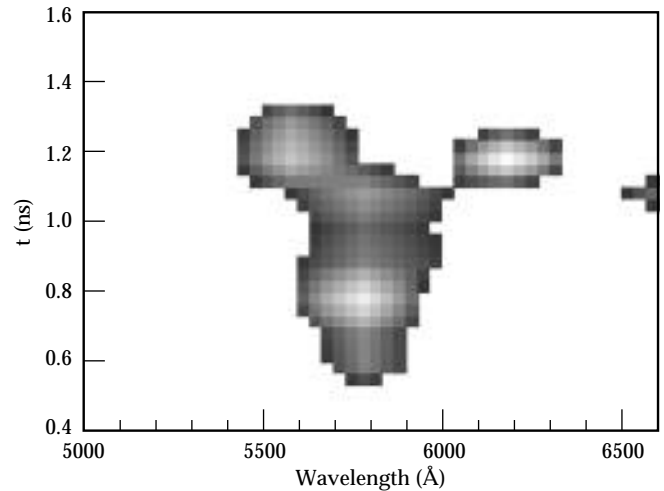


FIGURE 6. Calculated SRS backscattered spectra from a neopentane-filled gasbag target with $f/8$ interaction beam intensity $I = 2 \times 10^{15} \text{ W/cm}^2$. (50-04-1095-2382pb02)

these experiments quantitatively. The measured SBS reflectivities for these plasmas are well below the scattering levels predicted by linear theory. For the SBS gain exponents of >20 calculated for these conditions, the calculated reflectivity is limited by pump depletion to $\sim 30\%$ in the absence of other nonlinear saturation mechanisms, whereas the measured reflectivities are $<3\%$ in neopentane-filled targets.^{8,9} For these high gains, however, nonlinear saturation mechanisms that limit the amplitude or coherence of the ion waves driven by SBS^{3,21} are likely to be important. Theoretical and experimental efforts are under way to quantify these effects. Further, scattering from high- Z blowoff from the gold wall in NIF hohlraums is not well modeled in these Nova targets. Although gold plasma in the Nova gas-filled hohlraums may contribute to the SBS signal, tamping of the wall expansion reduces the extent of the high- Z blowoff, and strong absorption in the gas fill reduces the laser intensity in the high- Z plasma to below NIF-relevant levels. Scattering from high- Z plasmas is the subject of continuing research.

Conclusion

Using gas-filled targets on Nova, we have produced plasmas that closely match the calculated low- Z plasma environment in NIF hohlraums in electron density and temperature, density and velocity scalelengths, and calculated SBS gain. These plasmas were extensively characterized using x-ray and optical diagnostics. The plasma parameters and target evolution predicted by LASNEX design calculations are consistent with these observations. These comparisons verify that the desired parameters for SBS experiments were attained and corroborate important aspects of our modeling of NIF hohlraum conditions. SBS reflectivity is $<3\%$ from an interaction beam that mimics the NIF laser beam intensity, focusing, and beam smoothing.

Acknowledgments

We acknowledge valuable discussions with J. D. Kilkenny, J. D. Lindl, and M. D. Rosen, and the support of the LASNEX group in performing simulations required to design and analyze these experiments.

Notes and References

1. S. W. Haan, S. M. Pollaine, J. D. Lindl, L. J. Suter, et al., *Phys. Plasmas* 2, 2480 (1995).
2. J. M. Moody, H. A. Baldis, D. S. Montgomery, R. L. Berger, et al., *Phys. Plasmas* 2, 4285 (1995).
3. W. L. Kruer, *Phys. Fluids* 23, 1273 (1980).
4. H. A. Baldis, D. S. Montgomery, J. D. Moody, C. Labaune, et al., *Plasma Phys. Controlled Fusion* 34, 2077 (1992), and references therein.
5. C. A. Back, D. H. Kalantar, R. L. Kauffman, R. W. Lee, et al., "Measurements of electron temperature by spectroscopy in millimeter-size hohlraum targets," Lawrence Livermore National Laboratory, Livermore, CA, UCRL-JC-122046; submitted to *Phys. Rev. Lett* (1996).
6. D. H. Kalantar et al., *Phys. Plasmas* 2, 3161 (1995).
7. L. V. Powers, R. L. Berger, R. L. Kauffman, B. J. MacGowan, et al., *Phys. Plasmas* 2, 2473 (1995).
8. B. J. MacGowan, C. A. Back, R. L. Berger, K. S. Bradley, et al., *Proceedings of the IAEA 15th International Conference on Plasma Physics and Controlled Nuclear Fusion Research* (International Atomic Energy Agency, Vienna, 1994), p. 16.
9. L. V. Powers, R. E. Turner, R. L. Kauffman, R. L. Berger, et al., *Phys. Rev. Lett.* 74, 2957 (1995).
10. D. S. Montgomery et al., *Bull. Am. Phys. Soc.* 39, 1952 (1994).
11. B. J. MacGowan, R. Berger, J. Fernandez, B. Afeyan, et al., *ICF Quarterly Report* 5(4), 305, Lawrence Livermore National Laboratory, Livermore, CA, UCRL-LR-105821-95-4 (1995).
12. R. L. Berger, B. F. Lasinski, T. B. Kaiser, E. A. Williams, et al., *Phys. Fluids B* 5, 2243 (1993); R. L. Berger, T. B. Kaiser, B. F. Lasinski, C. W. Still, *ICF Quarterly Report* 5(3), 200–207, Lawrence Livermore National Laboratory, Livermore, CA, UCRL-LR-105821-95-3 (1995).
13. R. K. Kirkwood, B. B. Afeyan, W. L. Kruer, B. J. MacGowan, et al., "Observation of energy transfer between frequency mismatched laser beams in large scale plasma," Lawrence Livermore National Laboratory, Livermore, CA, UCRL-JC-122102; submitted to *Phys. Rev. Lett.* (1996).
14. G. Zimmerman and W. Kruer, *Comments Plasma Phys. Controlled Fusion* 2, 85 (1975).
15. D. W. Forslund, J. M. Kindel, and E. L. Lindman, *Phys. Fluids* 18, 1002 (1975); R. L. Berger, E. A. Williams, and A. Simon, *Phys. Fluids B* 1, 414 (1989).
16. E. A. Williams, R. L. Berger, A. V. Rubenchik, R. P. Drake, et al., *Phys. Plasmas* 2, 129 (1995); H. X. Vu, J. M. Wallace, and B. Bezzerides, *Phys. Plasmas* 1 (11), 3542–3556 (1994).
17. H. A. Rose and D. F. DuBois, *Phys. Rev. Lett.* 72, 2883 (1994).
18. R. L. Berger, B. F. Lasinski, A. B. Langdon, T. B. Kaiser, et al., *Phys. Rev. Lett.* 75, 1078 (1995).
19. J. Denavit and D. W. Phillion, *Phys. Plasmas* 1, 1971 (1994).
20. J. C. Fernandez, J. A. Cobble, B. H. Failor, W. W. Hsing, et al., 53 *Phys. Rev. E* (1996).
21. S. C. Wilks et al., *Phys. Rev. Lett.* 75, 5048 (1995); B. I. Cohen et al., *Bull. Am. Phys. Soc.* 40, 1778 (1995).